Structure of the Transition States and Intermediates Formed in the Water-Exchange of Metal Hexaaqua Ions of the First Transition Series

François P. Rotzinger

Contribution from the Institut de chimie physique II, Ecole Polytechnique Fédérale, CH-1015 Lausanne, Switzerland

Received January 19, 1996. Revised Manuscript Received May 7, 1996[⊗]

Abstract: The structures of the transition states and intermediates formed in the water-exchange of hexaaqua complexes of the first row transition elements have been computed with ab initio methods at the Hartree−Fock or CAS-SCF level. As an approximation, water molecules in the second coordination sphere except one, bulk water, and anions have been neglected. For each of the three types of activation, namely associative, concerted, and dissociative mechanism, a representative transition metal complex has been studied, viz. $Ti(OH_2)_6^{3+}$, $V(OH_2)_6^{2+}$, and $Ni(OH_2)_6^{2+}$. Each type of mechanism proceeds via a characteristic transition state. For the A and D mechanisms, respectively, hepta- or pentacoordinated intermediates are formed, and their lifetimes were estimated based on the energy difference between that of the transition state and the corresponding intermediate. The computed activation energies are in agreement with the experimental values and are independent of the mechanism or the charge on the metal center. The bond length changes occurring during the activation agree with the corresponding experimental $\Delta V^{\ddagger}$ values. In a recent article, Åkesson et al. (*J. Am. Chem. Soc.* **1994**, *116*, 8705) proposed an interpretation of the experimental $\Delta V^{\ddagger}$ values that differs from that commonly applied (Merbach, A. E. *Pure Appl. Chem.* **1987**, *59*, 161). In particular, they claimed a dissociative activation for the water-exchange of the hexaaqua ions of V^{II} and Mn^{II} in spite of their negative volumes of activation. The present computational results on V^{II} are in perfect agreement with the I_a mechanism attributed on the basis of its $\Delta V^{\ddagger}$ value. It should be noted that in principle, the D mechanism is possible for all the hexaaqua ions of the first transition series, but in many cases, the associative or concerted pathway is preferred. For a given complex, all the possible mechanisms must be analyzed, before the most favorable pathway can be determined. The presently studied case of V^{II}, where equal energies of activation have been computed for the I_a and D mechanism, illustrates this point. The attribution of the mechanism was only possible by comparison with the experimental volume of activation. Computed energies of activation alone may not suffice to identify the mechanism; a safe attribution can only be made if the structural changes agree with the volume of activation.

Introduction

Ligand substitutions and exchange involving a variety of metal ions and ligands have been reviewed recently by Lincoln and Merbach.[1] The most simple substitution process involving aqua complexes of transition metals is the water-exchange. The detailed knowledge of such reactions is, however, relevant not only for the understanding of the substitution mechanisms but also for the electron transfer proceeding via the inner-sphere pathway, since the latter is necessarily preceded by a substitution process.[2]

The substitution mechanisms are classified with the symbols A, I_a, I, I_d, and D, where A and D represent associative and dissociative mechanisms proceeding via hepta- or pentacoordinated intermediates, respectively, and I_a, I, or I_d describe concerted reactions that may have some associative (I_a) or dissociative (I_d) character.[3] The mechanisms are attributed based on thermodynamic activation parameters like $\Delta H^{\ddagger}$, $\Delta S^{\ddagger}$, $\Delta G^{\ddagger}$ or $\Delta V^{\ddagger}$. The volume of activation is generally accepted to be the strongest criterion: large negative values point toward an A and large positive values toward a D mechanism.[4] Smaller values are interpreted as an I mechanism. All these thermochemical parameters describe global or total phenomena, viz. every parameter describes the sum of the effects arising from the bulk solvent, the second coordination sphere solvent, and the transition metal complex itself. For water-exchange, the contribution due to the electrostriction of the second coordination sphere and bulk water is known to be small.[5] Therefore, the experimental $\Delta V^{\ddagger}$ values reflect mainly changes in the first coordination sphere which are investigated with the present calculations.

In a recent article, Sandström and co-workers[6] claimed that a dissociative rather than an associative mechanism operates for $V(OH_2)_6^{2+}$ and $Mn(OH_2)_6^{2+}$. It should be noted that their pentagonal bipyramidal heptacoordinated species of the type $M(OH_2)_7^{n+}$ have been computed with highly constrained optimizations, and furthermore, not a single frequency computation on such a species has been reported. According to the present calculations, Sandström's $M(OH_2)_7^{n+}$ species do not represent chemically relevant stationary points on the potential energy surface, and therefore, their mechanistic interpretations based on these species might be questionable. Our computations, however, are in perfect agreement with the I_a mechanism derived from measurements of the activation volumes.[7,8]

[⊗] Abstract published in *Advance ACS Abstracts,* July 1, 1996.

(1) Lincoln, S. F.; Merbach, A. E. *Adv. Inorg. Chem.* **1995**, *42*, 1.

(2) (a) Taube, H.; Myers, H.; Rich, R. L. *J. Am. Chem. Soc.* **1953**, *75*, 4118. (b) Taube, H. *Can. J. Chem.* **1959**, *37*, 129. (c) Taube, H. *Electron Transfer Reactions of Complex Ions in Solution*; Academic Press: New York, 1970.

(3) Langford, C. H.; Gray, H. B. *Ligand Substitution Dynamics*; Benjamin: New York, 1965.

(4) Swaddle, T. W. *Adv. Inorg. Bioinorg. Mech.* **1983**, *2*, 95.

(5) Merbach, A. E. *Pure Appl. Chem.* **1982**, *54*, 1479.

(6) Åkesson, R.; Pettersson, G. M.; Sandström, M.; Wahlgren, U. *J. Am. Chem Soc.* **1994**, *116*, 8705.

(7) Ducommun, Y.; Zbinden, D.; Merbach, A. E. *Helv. Chim. Acta* **1982**, *65*, 1385.

S0002-7863(96)00184-9 CCC: $12.00

In the present article, all the transition state and intermediate structures that could occur along the reaction coordinate of the water-exchange process involving representative hexaaqua ions of the 3d metals have been computed. Since there are three types of mechanisms, three typical examples are discussed in this study, together with their most favorable reaction pathways. Furthermore, the lifetime of one penta- and one heptacoordinated intermediate has been calculated. The structures of the transition states are related to the electronic structure or vice versa, and the correlation electronic structure−substitution mechanism is discussed.

The calculations have been performed with ab initio methods at the Hartree−Fock or CAS-SCF (complete active space SCF, a multiconfigurational approach) level where appropriate; dynamic electron correlation was neglected. The validity of this approximation has been verified using density functional theory. It should be noted that a transition state is characterized by a *single* imaginary vibrational frequency, whereas an intermediate has *no* imaginary frequency. Species with more than one imaginary frequency do not represent chemically relevant species on the potential energy surface. In this study, reactants, products, and intermediates are characterized by the absence of any imaginary frequency throughout, whereas transition states always have a single imaginary frequency.

As an approximation, second coordination sphere and bulk water as well as the anions have been neglected. Activation energies for the associative (A) and the concerted (I_a, I, I_d) pathways have been computed based on eq 1a, and for the dissociative (D) ones, both eqs 1a or 1b can be used. The bond length changes occurring during the activation were compared with the volumes of activation, and these changes, together with the structures of the transition states, allow the assignment of the mechanism.

$$[M(OH_2)_6 \cdot OH_2]^{n+} \rightarrow [M(OH_2)_7^{n+}]^{\ddagger} \quad (1a)$$

$$M(OH_2)_6^{n+} \rightarrow [M(OH_2)_6^{n+}]^{\ddagger} \quad (1b)$$

As mentioned above, one example for each type of mechanism is discussed: the associative, concerted, and dissociative activations have been analyzed based on the examples of $Ti(OH_2)_6^{3+}$, $V(OH_2)_6^{2+}$, and $Ni(OH_2)_6^{2+}$, respectively. Interestingly, each type of mechanism proceeds via a different transition state; the present results suggest that the structure of the transition states and intermediates provides a straightforward criterion for the attribution of the reaction mechanism. The calculated structural changes parallel the experimentally determined volumes of activation. To our knowledge, this is the first study discussing substitution mechanisms of transition metal aqua ions based on transition state and intermediate structures that were calculated with ab initio methods.

Results

Hexahydrates and Their Water Adducts. Åkesson et al. have shown that the computed geometries of the free (gas phase) $M(OH_2)_6^{n+}$ complexes are not the same as those found in crystal structures.[9] In the following calculations, dynamic electron correlation has been neglected, and the error due to this approximation has been estimated by comparing the bond lengths obtained at the Hartree−Fock level with those from density functional theory. The latter includes dynamic correlation, but it is not suitable for the treatment of species with nearly degenerate states (e.g. the doublet states of $[V(OH_2)_7^{2+}]^{\ddagger}$) requiring a CAS-SCF wave function. Although density functional theory would provide better results for a variety of compounds, since it includes dynamic correlation, a uniform treatment of all the elements of the first transition series is not possible at this level. For this reason, the computations have been performed at the Hartree−Fock or CAS-SCF level where necessary. The pertinent calculations for the $M(OH_2)_6^{n+}$ complexes are shown in Table 1. For $Ni(OH_2)_6^{2+}$, the same M−O bond lengths were obtained with density function theory and Hartree−Fock calculations. The bond lengths of $Ti(OH_2)_6^{3+}$ and $V(OH_2)_6^{2+}$ were, however, slightly longer in the Hartree−Fock calculations. This relatively small error is due to the omission of dynamic correlation.

Calculations on the water adducts $[M(OH_2)_6 \cdot OH_2]^{n+}$ clearly show that the M−O bond lengths obtained for $M(OH_2)_6^{n+}$ complexes are too long. This arises from the omission of the second coordination sphere water molecules and possibly the anions, since the M−O bond of the water ligand carrying the second coordination sphere water is shorter than the others by at least 0.05 Å (Table 1). The geometry optimizations have been performed in C_1 symmetry for V^{II} and Ni^{II}, and the symmetry was found to be C_s. Therefore, the adduct $[Ti(OH_2)_6 \cdot OH_2]^{3+}$ has then been computed in C_s symmetry. A perspective view of this species is shown in Figure 1. It should be noted that for the present exchange reactions, the water adducts represent either the reactant or the product.

Transition States. For the two aqua ions $Ti(OH_2)_6^{3+}$ and $Ni(OH_2)_6^{2+}$, the most negative and the most positive volumes of activation have been measured,[8,10] respectively, whereas for $V(OH_2)_6^{2+}$ an intermediate value has been observed[7] (Table 2). Interestingly, the corresponding three water-exchange reactions proceed via quite disparate transition states. The $\{[Ti(OH_2)_6 \cdots OH_2]^{3+}\}^{\ddagger}$ species has C_1 symmetry, and the incoming ligand can be recognized easily (Figure 2). The imaginary mode describes an almost pure motion of the entering ligand toward or away from the Ti^{III} center. In this reaction, water entry dominates clearly the activation process, since the six M−O bonds of $Ti(OH_2)_6^{3+}$ do not alter appreciably, when the single second coordination sphere water molecule penetrates into the first coordination sphere (Table 1a). During this process, the pertinent M−O distance has been shortened by 1.3 Å from 4.13 Å to 2.81 Å. This transition state is typical for an A mechanism.

In contrast to the previous example, the transition state $\{[V(OH_2)_5 \cdots (OH_2)_2]^{2+}\}^{\ddagger}$, arising from a concerted process, has C_2 symmetry (Figure 3); the entering and leaving water molecules are symmetrically equivalent and indistinguishable, and the reaction coordinate is a *b* species (non totally symmetric). The bond lengths of the incoming or leaving water ligand are both 2.68 Å. This value is perfectly consistent with a concerted substitution mechanism, where entry of one ligand is accompanied by the stretching of the corresponding M−O bond of the leaving group. In fact, the imaginary mode describes the concerted shortening of one and the elongation of the other V−O bond involved in the exchange reaction. In this case, bond formation is more important than bond breaking, since the water in the second coordination sphere at 4.38 Å comes closer to the V^{II} center by 1.7 Å while the bond of the leaving ligand is elongated by only about 0.5 Å. The computed transition state structure is in perfect agreement with the I_a mechanism derived from the experimental volume of activation.[7] Another "transition state" with C_{2v} symmetry, a (distorted) pentagonal bipyramid, has also been located (Figure 4), but this

(8) Ducommun, Y.; Newman, K. E.; Merbach, A. E. *Inorg. Chem.* **1980**, *19*, 3696.

(9) Åkesson, R.; Pettersson, G. M.; Sandström, M.; Wahlgren, U. *J. Am. Chem Soc.* **1994**, *116*, 8691.

(10) Hugi, A. D.; Helm, L.; Merbach, A. E. *Inorg. Chem.* **1987**, *26*, 1763.

(11) Probst, M. M.; Hermansson, K. *J. Chem. Phys.* **1992**, *96*, 8995.

Table 1. Selected Properties of Reactants/Products, Transition States, and Intermediates[a]

species	electronic state (symmetry)	energy, au	d(M−O), Å	Σ[d(M−O)], Å
		(a) Complexes of Ti^{III}		
$Ti(OH_2)_6^{3+}$	$^2B_{1g}$ (D_{2h})	−2.297872[b]	2.09, 2.09, 2.09,2.09, 2.17, 2.17	12.70
$Ti(OH_2)_6^{3+}$	$^2B_{1g}$ (D_{2h})	−512.800990	2.11, 2.11, 2.12, 2.12, 2.16, 2.16	12.78
$[Ti(OH_2)_6{\cdot}OH_2]^{3+}$	$^2A''$ (C_s)	−588.866969	2.04, 2.12, 2.13, 2.13, 2.17, 2.17, 4.13	16.89
$\{[Ti(OH_2)_6\cdots OH_2]^{3+}\}^{‡}$	^2A (C_1)	−588.853581	2.17, 2.17, 2.16, 2.14, 2.11, 2.11, 2.81	15.67
$[Ti(OH_2)_7^{3+}]^{‡}$	^2B (C_2)	−588.857848	2.14, 2.14,2.22, 2.22, 2.21, 2.21, 2.21	15.35
$Ti(OH_2)_7^{3+}$	^2A (C_1)	−588.858554	2.13, 2.16, 2.17, 2.19, 2.21, 2.23, 2.25	15.34
$[Ti(OH_2)_5{\cdot}(OH_2)_2]^{3+}$	$^2B_2$ (C_{2v})	−588.832249	2.03, 2.03, 2.08, 2.15, 2.15, 4.03, 4.03	18.50
		(b) Complexes of V^{II}		
$V(OH_2)_6^{2+}$	^4A_g (T_h)[c]	−2.885815[b]	2.17[b,d]	13.02
$V(OH_2)_6^{2+}$	^4A_g (T_h)	−526.558701	2.21[d]	13.26
$\{[V(OH_2)_5\cdots OH_2]^{2+}\}^{‡}$	$^4A'$ (C_s)	−526.536626	2.15, 2.18, 2.18, 2.18, 2.21, 3.63	14.53
$[V(OH_2)_5{\cdot}OH_2]^{2+}$	$^4A'$ (C_s)	−526.537111	2.15, 2.18, 2.18, 2.18, 2.21, 4.20	15.10
$[V(OH_2)_6{\cdot}OH_2]^{2+}$	$^4A'$ (C_s)[e]	−602.600249	2.18, 2.21, 2.22, 2.22, 2.21, 2.21, 4.38	17.63
$\{[V(OH_2)_5\cdots(OH_2)_2]^{2+}\}^{‡}$	^4A (C_2)	−602.578190	2.21, 2.21, 2.22, 2.22, 2.23, 2.68, 2.68	16.45
$[V(OH_2)_5\cdots(OH_2)_2]^{2+}$[f]	$^4B_1$ (C_{2v})	−602.574029	2.61, 2.61, 2.36, 2.21, 2.21, 2.22, 2.22	16.44
$[V(OH_2)_7^{2+}]^{‡}$	^2A (C_2)	−602.508126	2.23, 2.23, 2.29, 2.29, 2.26, 2.39, 2.39	16.08
$[V(OH_2)_7^{2+}]^{‡}$	^2B (C_2)	−602.507244	2.29, 2.29, 2.25, 2.25, 2.27, 2.35, 2.35	16.05
		(c) Complexes of Ni^{II}		
$Ni(OH_2)_6^{2+}$	^3A_g (T_h)[c]	−2.686839[b]	2.11[b,d]	12.66
$Ni(OH_2)_6^{2+}$	^3A_g (T_h)	−624.234910	2.11[d]	12.66
$\{[Ni(OH_2)_5\cdots OH_2]^{2+}\}^{‡}$	$^3A'$ (C_s)	−624.217043	2.05, 2.07, 2.07, 2.07, 2.10, 3.38	13.74
$[Ni(OH_2)_5{\cdot}OH_2]^{2+}$	$^3A'$ (C_s)	−624.218375	2.04, 2.07, 2.07, 2.07, 2.11, 4.17	14.53
$[Ni(OH_2)_6{\cdot}OH_2]^{2+}$	$^3A'$ (C_s)[e]	−700.277398	2.07, 2.12, 2.12, 2.12, 2.12, 2.12, 4.28	16.95
$\{[Ni(OH_2)_5\cdots OH_2{\cdot}OH_2]^{2+}\}^{‡}$	$^3A'$ (C_s)	−700.261055	2.05, 2.05, 2.08, 2.08, 2.08, 3.34, 4.27	17.95
$[Ni(OH_2)_5{\cdot}(OH_2)_2]^{2+}$	$^3A_1$ (C_{2v})	−700.262834	2.05, 2.05, 2.08, 2.07, 2.07, 4.22, 4.22	18.76
$[Ni(OH_2)_5\cdots(OH_2)_2]^{2+}$[f]	$^3B_1$ (C_{2v})	−700.251605	2.09, 2.09, 2.06, 2.06, 2.14, 3.06, 3.06	16.56

[a] Hartree-Fock or CAS-SCF calculations, unless noted otherwise. [b] Computation using density functional theory (see Computational Details). [c] Computation using D_{2h} symmetry. [d] All six bonds have the same length. [e] Computation using C_1 symmetry. [f] Hyper saddel point with two imaginary frequencies.

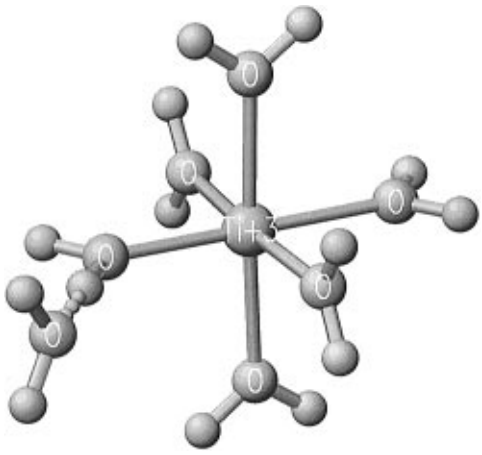

Figure 1. Perspective view of the $[Ti(OH_2)_6{\cdot}OH_2]^{3+}$ water adduct.

species has *two imaginary frequencies* and hence it is a hyper saddle point having no relevance for the water-exchange. Furthermore, its energy is significantly higher (Tables 1b and 2) than that of the true transition states (see above and below). An analogous species, exhibiting also two imaginary frequencies and a high energy, has also been found for Ni^{II} (Table 1c). The latter two resemble the heptacoordinated species that have been investigated by Åkesson et al.[6]

Attempts to compute a transition state for an associative or concerted pathway for the water-exchange of $Ni(OH_2)_6^{2+}$ failed, but a transition state was found readily for the dissociative activation. This species, $\{[Ni(OH_2)_5\cdots OH_2{\cdot}OH_2]^{2+}\}^{‡}$, carrying also a second coordination sphere water molecule, is quite different from the two previous ones (Figure 5): it has C_s symmetry, the "incoming" and departing ligands are well distinguishable. The imaginary mode involves mainly a motion of the leaving ligand toward or away from the Ni^{II} center. Here, the activation is dominated by ligand loss: the M−O bond of the leaving water molecule is elongated by 1.2 Å while the other five bonds and also the M−O distance of the second coordination sphere water (the "incoming" ligand) remain nearly unchanged. Although the water molecule in the second sphere is close to the leaving ligand and the generated vacant site, it does not show any tendency to occupy the place of the latter (Figure 5, Table 1c). The structure of this transition state shows that a dissociative activation is not affected by ligands in the second coordination sphere. This observation was corroborated by the computation of the transition state with the second sphere water molecule omitted: the structures of the two transition states are very similar, in particular the bond length of the leaving ligand (Table 1c, Figures 5 and 6).

The dissociative pathway has also been investigated in detail for V^{II}, where the computation has been done by omitting the "inactive" second coordination sphere water molecule. In the transition state $\{[V(OH_2)_5\cdots OH_2]^{2+}\}^{‡}$ (Table 1b) with C_s symmetry, the V−O bond has been elongated by about 1.4 Å, and the leaving ligand is also attracted by the closest hydrogen atom of an equatorial water ligand as in the corresponding Ni^{II} compound (Figure 6). In the V^{II} case, the energy of activation for the I_a and D mechanism is the same (Tables 1b and 2), but the structural changes relating to the volume of activation are quite different.

It is obvious that the three different types of activation, namely the associative, concerted, or dissociative, give rise to structurally quite disparate and characteristic transition states (Figures 2, 3, 5, and 6).

Intermediates. In principle, all the transition states with symmetry-inequivalent incoming and leaving ligands must ultimately be followed by intermediates where the entering and departing ligands are symmetry equivalent. Therefore, the water-exchange of $Ti(OH_2)_6^{3+}$ and $Ni(OH_2)_6^{2+}$ has to involve intermediates. The heptacoordinated intermediate $Ti(OH_2)_7^{3+}$ (Figure 7) has nearly C_2 symmetry and resembles the transition state of V^{II} (Figure 3) very much, but it has *only real vibrational frequencies* in contrast to the latter having an imaginary one.

Table 2. Energy and Bond Length Differences Relative to the Corresponding $M(OH_2)_6^{n+}$ Complexes or Their Respective $[M(OH_2)_6 \cdot OH_2]^{n+}$ Water Adducts—Comparison with Experimental Data[a]

species[b]	$\Delta H^{\ddagger}$ [c]	$\Delta S^{\ddagger}$ [d]	$\Delta G^{\ddagger}_{298}$ [c]	ΔE or $\Delta E^{\ddagger}$ [c,e]	$\Delta V^{\ddagger}$ [f]	$\Delta\Sigma$[g]
$\{[Ti(OH_2)_6 \cdots OH_2]^{3+}\}^{\ddagger}$	43.4	+1.2	43.0	35.2	−12.1	−1.22
$Ti(OH_2)_7^{3+}$				22.1		−1.55
$[Ti(OH_2)_5 \cdot (OH_2)_2]^{3+}$				91.2		+1.61
$\{[V(OH_2)_5 \cdots OH_2]^{2+}\}^{\ddagger}$	61.8	−0.4	61.9	58.0	−4.1	+1.27
$[V(OH_2)_5 \cdot OH_2]^{2+}$				56.7		+1.84
$\{[V(OH_2)_5 \cdots (OH_2)_2]^{2+}\}^{\ddagger}$	61.8	−0.4	61.9	57.9	−4.1	−1.18
$[V(OH_2)_5 \cdots (OH_2)_2]^{2+}$ [h]				68.8		−1.19
$[V(OH_2)_7^{2+}]^{\ddagger}$ [i]				242		−1.55
$[V(OH_2)_7^{2+}]^{\ddagger}$ [j]				244		−1.58
$\{[Ni(OH_2)_5 \cdots OH_2]^{2+}\}^{\ddagger}$	56.9	+32.0	47.4	46.9	+7.2	+1.08
$[Ni(OH_2)_5 \cdot OH_2]^{2+}$				43.4		+1.87
$\{[Ni(OH_2)_5 \cdots OH_2 \cdot OH_2]^{2+}\}^{\ddagger}$	56.9	+32.0	47.4	42.9	+7.2	+1.00
$[Ni(OH_2)_5 \cdot (OH_2)_2]^{2+}$				38.2		+1.81
$[Ni(OH_2)_5 \cdots (OH_2)_2]^{2+}$ [h]				67.7		−0.39

[a] References 7, 8, and 10. [b] The ΔE, $\Delta E^{\ddagger}$ or $\Delta\Sigma$ values for species with 6 or 7 H_2O molecules are based on the respective reactants with the same amount of H_2O. [c] Units: kJ/mol. [d] Units: J K^{-1} mol^{-1}. [e] No zero point energy has been included. [f] Units: cm^3/mol. [g] $\Delta\Sigma$ = difference between the $\Sigma[d(M-O)]$ entries from Table 1, e. g. $\Delta\Sigma = \Sigma[d(M-O)]\{\text{transition state/intermediate}\} - \Sigma[d(M-O)]\{M(OH_2)_6^{n+}/[M(OH_2)_6 \cdot OH_2]^{n+}\}$; units: Å. [h] Hyper saddle point (two imaginary frequencies). [i] ^{2}A state. [j] ^{2}B state.

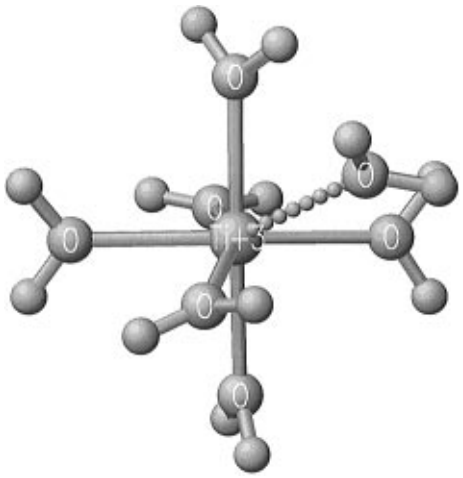

Figure 2. Perspective view of the $\{[Ti(OH_2)_6 \cdots OH_2]^{3+}\}^{\ddagger}$ transition state.

Also, it should be noted that all seven M−O bonds have approximately the same length (Table 1a, Figure 7). A similar structure, obtained with constrained optimizations, has been reported by Probst et al. for $M(OH_2)_7^{n+}$ complexes (M = Li^+, Na^+, Mg^{2+}, and Al^{3+}).[11] Since the $Ti(OH_2)_7^{3+}$ intermediate has C_1 symmetry, the incoming and leaving ligands are symmetry inequivalent. Water-exchange can only take place if at one stage of the substitution process the incoming and leaving ligand become (symmetrically) equivalent. In this case, this occurs via the transition state $[Ti(OH_2)_7^{3+}]^{\ddagger}$ having C_2 symmetry (Table 1a, Figure 8). The latter species, exhibiting necessarily an imaginary frequency, is very difficult to distinguish from the intermediate $[Ti(OH_2)_7]^{3+}$ (Figure 7). The reaction coordinate, a *b* species, involves mainly rotations of two water ligands, and the energy of activation for this doubtless very fast process is about 1.9 kJ/mol (Table 1a).

In all the heptacoordinated species, regardless whether they are intermediates or transition states, one d_π (t_{2g} in O_h symmetry) orbital is destabilized, and for this reason, doublet states of e.g. V^{II} or Cr^{III} in which 3 electrons occupy the two lowest 3d orbitals have to be considered. The geometries of the two $V(OH_2)_7^{2+}$ species with C_2 symmetry in their respective ^{2}A and ^{2}B states have been optimized. These calculations required CAS-SCF wave functions, and the thus obtained species (Table 1b) are the V^{II} analogs of the previously discussed $[Ti(OH_2)_7^{3+}]^{\ddagger}$ transition state (Table 1a, Figure 8): the (single) imaginary mode is not related to the reaction coordinate for water-exchange, but

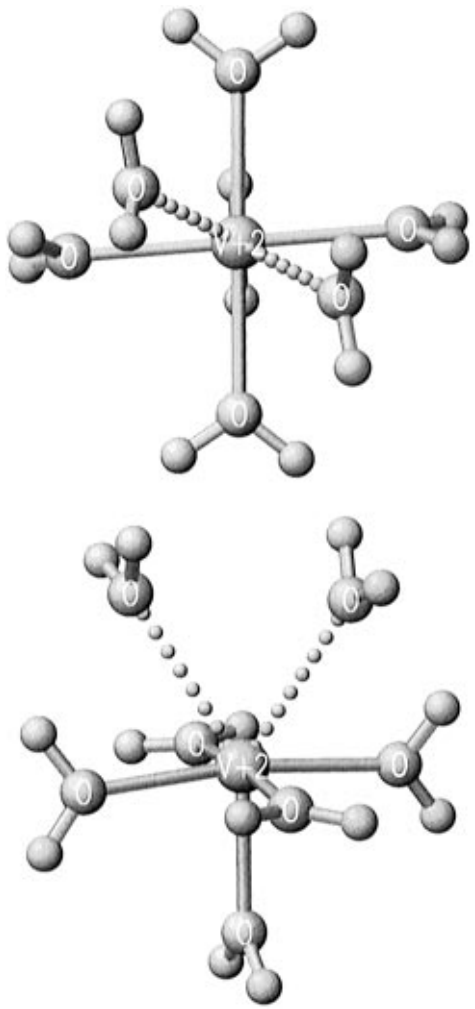

Figure 3. Transition state $\{[V(OH_2)_5 \cdots (OH_2)_2]^{2+}\}^{\ddagger}$ with C_2 symmetry: (a) view along the C_2 axis; (b) perspective view.

describes, as in the previously discussed Ti^{III} case, the interconversion of the two (enantiomeric) intermediates having C_1 symmetry. The V^{II} analogs of the latter intermediates have not been computed, since they are expected to be structurally only slightly different from the computationally much less demanding transition state with C_2 symmetry, and furthermore, their energy is expected to be lower by only about 2 kJ/mol (see above). The transition states $[V(OH_2)_7^{2+}]^{\ddagger}$ (^{2}A and ^{2}B states, C_2 symmetry) exhibit a very high energy (+242 and +244 kJ/mol

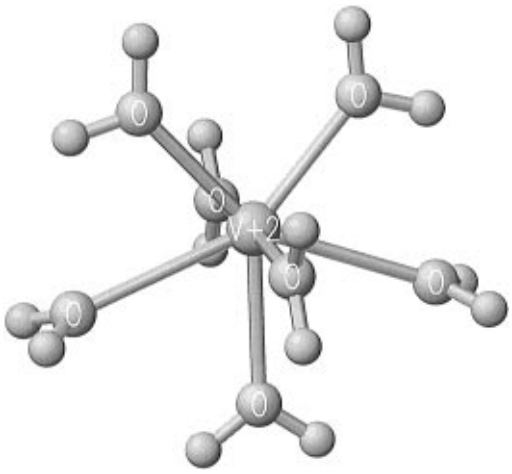

Figure 4. Perspective view of the pentagonal bipyramidal hyper saddle point species $\{[V(OH_2)_5\cdots(OH_2)_2]^{2+}\}^{\ddagger}$ with C_{2v} symmetry.

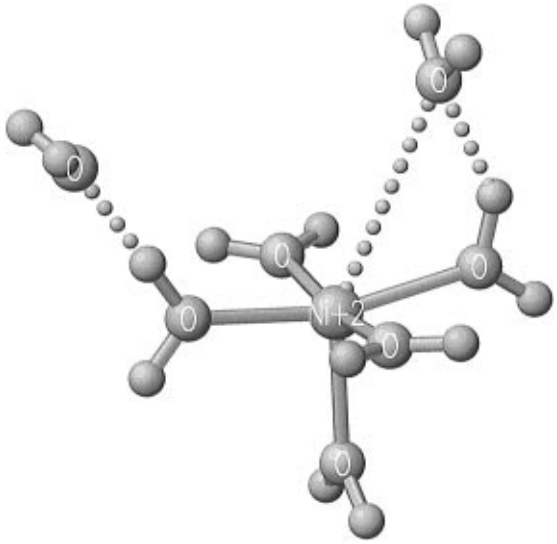

Figure 5. Perspective view of the $\{[Ni(OH_2)_5\cdots OH_2\cdot OH_2]^{2+}\}^{\ddagger}$ transition state.

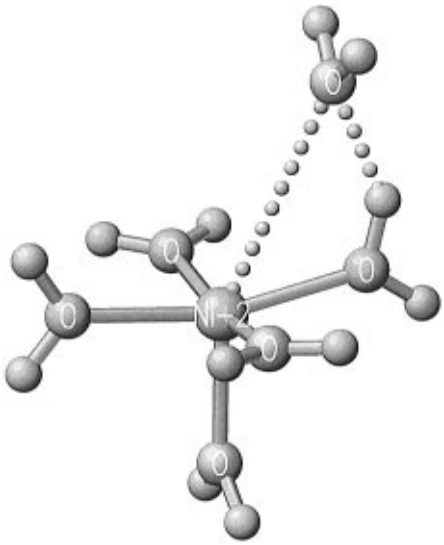

Figure 6. Perspective view of the $\{[Ni(OH_2)_5\cdots OH_2]^{2+}\}^{\ddagger}$ transition state.

relative to $[V(OH_2)_6\cdot OH_2]^{2+}$ for the ^2A and ^2B states, respectively) and V−O bonds that are substantially shorter than those of the transition state $\{[V(OH_2)_5\cdots(OH_2)_2]^{2+}\}^{\ddagger}$ with a quartet state which is formed in the concerted pathway (Table 1b). This

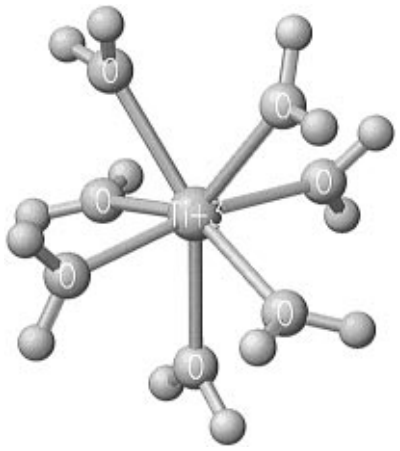

Figure 7. Perspective view of the heptacoordinated intermediate $Ti(OH_2)_7^{3+}$ with C_1 symmetry.

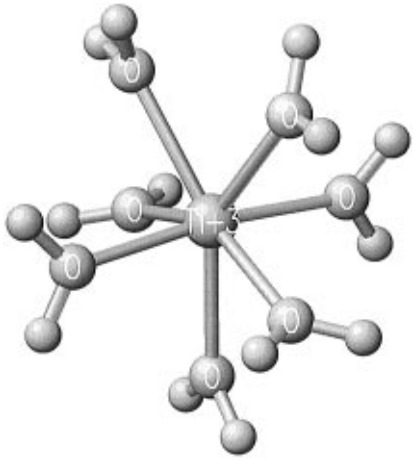

Figure 8. Perspective view of the transition state $\{[Ti(OH_2)_7]^{3+}\}^{\ddagger}$ with C_2 symmetry that equivalences the incoming and leaving water ligands.

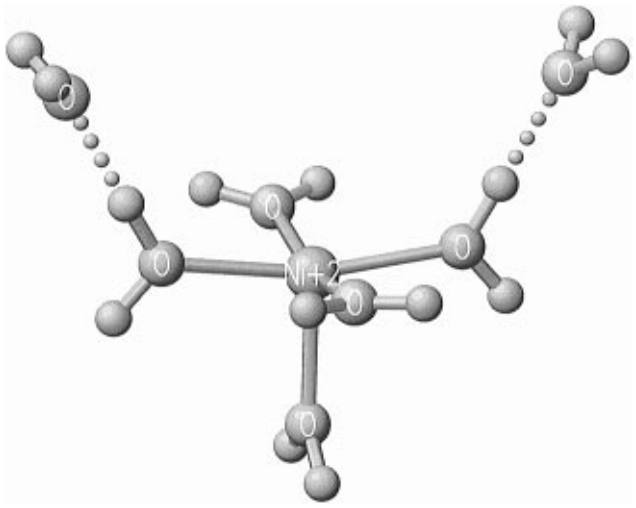

Figure 9. Perspective view of the pentacoordinated square-pyramidal intermediate $[Ni(OH_2)_5\cdot(OH_2)_2]^{2+}$.

calculation shows that it can be excluded that any species of V^{II} in the doublet state participates in the water-exchange.

The intermediate $[Ni(OH_2)_5\cdot(OH_2)_2]^{2+}$ has C_{2v} symmetry (Figure 9). Basically, it is a square pyramidal pentacoordinated species being hydrated by two water molecules. The leaving water ligand (Figure 5) has escaped into the second coordination sphere where it is symmetry equivalent with the other (the "incoming") second coordination sphere water. Remarkably, the energies of both intermediates $[Ni(OH_2)_5\cdot(OH_2)_2]^{2+}$ and [Ni-

$(OH_2)_5 \cdot OH_2]^{2+}$ are close to those of their respective transition states (Table 1c).

The dissociative pathway has also been analyzed for Ti^{III}. Since for such an activation the energy of the transition state and the corresponding intermediate are very close as shown above, only the computationally less demanding intermediate $[Ti(OH_2)_5 \cdot (OH_2)_2]^{3+}$ (resembling that represented in Figure 9) has been calculated (Table 1a). Although its energy has to be slightly lower than that of its preceding transition state, it is considerably higher (Table 2) than that of the transition state $\{[Ti(OH_2)_6 \cdots OH_2]^{3+}\}^{\ddagger}$ for the A mechanism. Therefore, the dissociative pathway can be ruled out for Ti^{III}.

Energies and total bond length changes in comparison to the respective $M(OH_2)_6^{n+}$ complexes or their $[M(OH_2)_6 \cdot OH_2]^{n+}$ water adducts are summarized in Table 2.

Discussion

As already mentioned in the introduction, most of the present calculations have been performed at the Hartree−Fock level. In general, the 3d electrons of the transition elements are correlated, and therefore, CAS-SCF calculations are required. Many of the selected examples, however, have very weakly correlated 3d electrons: the single 3d electron of Ti^{III} cannot be correlated to another one, and both V^{II} (in the quartet state) and Ni^{II} have either filled or half-filled or empty d_π or d_σ^* subshells. In these cases, there is no near degeneracy, and states arising from $d_\pi \rightarrow d_\sigma^*$ excitations are irrelevant as checked by CI calculations ($C_{HF} > 0.997$). Hence, Hartree−Fock wave functions were adequate for all these V^{II} and Ni^{II} complexes. The doublet states of V^{II}, however, required a CAS-SCF wave function.

The agreement between experimental $\Delta G^{\ddagger}$ (or $\Delta H^{\ddagger}$) and calculated $\Delta E^{\ddagger}$ values is good, if not excellent. This supports the validity of the model represented by eq 1 and the structures of the transition states. Zero point energies have not been included in $\Delta E^{\ddagger}$ and ΔE, because much more severe approximations like the omission of all the second coordination sphere water molecules except one, the bulk water, and the counterions have already been made.

The lifetime of the intermediates can be estimated based on the corresponding $\Delta E^{\ddagger}$ and ΔE values from Table 2 by computing the energy of activation ($\Delta E_I^{\ddagger}$) for the process described by eq 2.

$$\text{intermediate} \rightarrow \text{transition state} \qquad (2)$$

For the intermediates $Ti(OH_2)_7^{3+}$ and $[Ni(OH_2)_5 \cdot (OH_2)_2]^{2+}$ or $[Ni(OH_2)_5 \cdot OH_2]^{2+}$, the corresponding lifetimes (τ) of the order of 2 ns, 40 ps, or 70 ps have been estimated based on eq 3.[12]

$$\tau = 1/k$$

$$k = Z \exp\{-\Delta E_I^{\ddagger}/RT\}$$

$$Z \approx 10^{11}\ s^{-1} \qquad (3)$$

Of course, the different lifetimes of the two intermediates $[Ni(OH_2)_5 \cdot (OH_2)_2]^{2+}$ and $[Ni(OH_2)_5 \cdot OH_2]^{2+}$ are an artifact arising from the different number of second coordination sphere water molecules considered in the calculation. Overall, it can be concluded that the $Ti(OH_2)_7^{3+}$ intermediate is quite long lived; its lifetime should be comparable to that of the pentacoordinated intermediate $Co(NHCH_3)(NH_2CH_3)_4^{2+}$ generated in the base hydrolysis of $Co(NH_2CH_3)_5X^{n+}$ complexes.[13] The pentacoordinated Ni^{II} species are very short lived; however, their lifetime is just sufficiently long for their participation in diffusion-controlled reactions. It is possible that the D mechanism obtained for Ni^{II} arises from the limitations of the present model. It remains to be verified whether the pentacoordinated intermediate becomes a transition state when an improved model including for example 12 water molecules in the second coordination sphere is used. In this case, water-exchange would proceed via the I_d mechanism.

For each of the three representative metal aqua ions, the computation of the transition states for the A, I_d...I...I_a, and D mechanisms has been attempted. For Ti^{III} the A and D and for V^{II} the I_a and D mechanisms are feasible whereas for Ni^{II}, only the dissociative pathway appeared to be viable (Tables 1 and 2). For Ti^{III} the energy of activation for the dissociative process is so high that this pathway can be ruled out. The activation energies for the I_a and D mechanism of V^{II}, however, are equal (Table 2), and therefore, the computed $\Delta E^{\ddagger}$ values do not allow the attribution of the mechanism.

The present computations supply also structural information which can be correlated with the experimental volumes of activation. The M−O bond lengths and their sum, viz. $\Sigma[d(M-O)]$, are reported in Table 1. The elongation or compression of a given bond during the activation usually affects also the other "spectator" bonds. For this reason, the changes of all the bond lengths or their sum, abbreviated with $\Delta\Sigma$ (Table 2), is expected to be related to the volume of activation. Table 2 shows that the sign of $\Delta\Sigma$ agrees with that of $\Delta V^{\ddagger}$, and in the case of V^{II} where the computed $\Delta E^{\ddagger}$ value did not allow the I_a mechanism to be distinguished from the D mechanism, the $\Delta\Sigma$ value for the I_a mechanism parallels the experimental volume of activation.[7] Åkesson et al.[6] questioned the commonly applied[14] interpretation of experimental $\Delta V^{\ddagger}$ values and claimed that the aqua ions of V^{II} and Mn^{II} undergo a dissociative substitution. Interestingly, Powell et al.[15] calculated approximate volumes of activation based on the computations of Åkesson et al.[6] and showed that they agree with the experimental $\Delta V^{\ddagger}$ values hence corroborating an associative activation for V^{II} and Mn^{II}. In the following discussion, Åkesson et al.'s[6] data are analyzed critically and compared with the present results.

First, the dissociative mechanism is discussed: Åkesson et al.[6] found a linear relationship of ΔE_6 vs log k_{ex} (k_{ex}: rate of water exchange) for V^{II}, Cr^{II}, Mn^{II}, Co^{II}, Ni^{II}, Cu^{II}, and Zn^{II}, where ΔE_6 is the energy for the dissociation of a water ligand from the $M(OH_2)_6^{2+}$ complex to form $M(OH_2)_5^{2+}$ and a free water ligand. Since the linear correlation held also for V^{II} and Mn^{II}, they concluded that these aqua ions undergo a dissociatively activated water exchange. The present calculations on V^{II} have shown, however, that the $\Delta E^{\ddagger}$ values for a D and I_a mechanism are equal and hence the computed energy of activation cannot be considered as a reliable quantity for the assignment of the mechanism. It should further be noted that the ΔE_6 values were not computed for transition states, but for pentacoordinated species that are most likely intermediates. The present study shows (Table 2) that for a dissociative reaction the energies of the transition state and the corresponding intermediate are very similar. This is the reason why Åkesson et al.[6] obtained the linear relationship. The latter allows the conclusion that for the above metal ions, the *dissociative mechanism could be possible*, but it does not exclude the operation of another mechanism.

For the associative activation, however, the situation is quite different: for the 3+ ions, Åkesson et al.[6] observed a linear relationship of ΔE_7 vs log k_{ex} with too large a slope, whereas

(12) Sutin, N. *Prog. Inorg. Chem.* **1983**, *30*, 441.
(13) Rotzinger, F. P. *Inorg. Chem.* **1991**, *30*, 2763.
(14) Merbach, A. E. *Pure Appl. Chem.* **1987**, *59*, 161.
(15) Powell, D. H.; Furrer, P.; Pittet, P.-A.; Merbach, A. E. *J. Phys. Chem.* **1995**, *99*, 16622.

for the 2+ ions, no correlation was found at all (ΔE_7 represents the dissociation energy of the heptacoordinated species into the hexacoordinated one and a free water molecule). Quite obviously, their model is inadequate for the description of the associative activation. This is because Åkesson et al.'s[6] seven coordinated species are structurally and also energetically quite different from the transition states computed in the present study; their seven-coordinated species were obtained in highly constrained optimizations and do not represent stationary points on the potential energy surface. In fact, they did not report any frequency computations that would be required for the characterization of the nature of the computed species. More generally, seven-coordinated intermediates and seven-coordinated transition states were not distinguished, i.e. they did not account for the structural variety of seven-coordinated species. The present calculations show that for Ti^{III} a seven-coordinated transition state and a seven coordinated intermediate exist, whereas for V^{II} there is only a structurally different seven-coordinated transition state, and this is precisely the distinction between the A and I_a mechanism. Furthermore, it should be noted that Ni^{II} does not form any seven-coordinated transition state or intermediate; such species have more than one imaginary frequency and therefore do not represent chemically relevant points on the potential energy surface (Tables 1 and 2).

The variations of $\Delta V^{\ddagger}$ with the nature of M in $M(OH_2)_6^{n+}$ complexes have been rationalized in terms of a More O'Ferrall type diagram,[14,16−18] where the limiting A or D mechanisms are suggested to give rise to $\Delta V^{\ddagger} = -13.5$ or $+13.5$ cm^3/mol, respectively. A water molecule in the first coordination sphere of any metal with any charge has a molar volume of 13.5 ± 1.0 cm^3/mol.[14,19]

The present calculations show why the limiting values of -13.5 or $+13.5$ cm^3/mol are not reached in the water-exchange of the aqua ions of the first transition series. The above limiting values apply most likely to the hepta- or pentacoordinated *intermediates*, but not to the *transition states*. The $\Delta V^{\ddagger}$ values, however, describe the volume change required to reach the *transition state which precedes the intermediate*. In the transition state, the entry or the loss of the ligand is not completed. The calculated $\Sigma[d(M-O)]$ and $\Delta\Sigma$ values (Tables 1 and 2) illustrate this point: in the substitution involving $Ti(OH_2)_6^{3+}$ the entering ligand is at 2.8 Å from the Ti^{III} center in the transition state, but at 2.2 Å in the intermediate, showing that indeed the *entry of the ligand is incomplete in the transition state*. The analysis of the $\Sigma[d(M-O)]$ values (Table 1a) reveals that the transformation of the transition state into the intermediate brings a further reduction of $\Sigma[d(M-O)]$ (by 0.35 Å).

Similar considerations are also valid for the dissociative processes that are discussed on the basis of the Ni^{II} example: the activated Ni−O bond in the transition state is about 3.3−3.4 Å long, whereas in the pentacoordinated intermediate it has reached 4.2 Å. In this case, the transition state is about half the way in between the reactant (with $d(Ni-O) = 2.1$ Å) and the intermediate, and consequently, the volume of activation of 7.2 cm^3/mol is approximately half of the limiting value of 13.5 ± 1.0 cm^3/mol.

The determination of the reaction mechanism using quantum chemical methods requires the explicit computation of the transition states for every possible reaction mechanism. Based on these obtained energies and volumes of activation, then only is the assignment of the mechanism possible. Assignments based on only the energy or only the volume of activation may lead to erroneous conclusions. I wish to emphasize, however, that in the present study two approximations have been made: in the molecular model, the anions, the second coordination sphere water molecules except one, and the bulk water have been neglected, and in the computations, dynamic electron correlation has not been included. The computations on the other elements of the first transition series will be reported later.

Computational Details

All the calculations have been performed on Cray Y-MP/M94 and HP 9000/735 computers using the GAMESS[20] or ADF 1.1.4 (Department of Theoretical Chemistry, Vrije Universiteit, Amsterdam)[21] programs.

For the (spin unrestricted) density functional calculations basis sets IV of the ADF package were taken (they are approximately of triple-ζ valence + polarization function quality). The local exchange-correlation functional of Vosko−Wilk−Nusair[22] and nonlocal corrections to the exchange and the correlation of Becke[23] and Perdew,[24] respectively, were used.

In the ab initio calculations, the basis sets of Stevens, Basch, Krauss, and Jasien[25] were used for the transition metals, where the 1s, 2s, and 2p shells are represented by relativistic effective core potentials, and the 3s, 3p, 4s, and 4p shells have double-ζ and the 3d triple-ζ quality. For O and H 6-31G(d) basis sets[26] were used ($\alpha_{3d} = 1.20$[27]).

All the ab initio calculations were first carried out at the restricted open shell Hartree−Fock level. Then, a singles−doubles CI involving the 3d orbitals and the entire virtual space was performed with C_1 symmetry for at least two states. If the coefficient of the HF wave function was <0.99 and/or the second state was of the same symmetry and close (<0.5 eV) to the first one, the final result was computed at the CAS-SCF level. In cases where several electronic states exist, they all have been computed, but only the lowest state is reported.

Location of the Transition States. Since, in general, this task can turn out to be quite difficult, the presently adopted procedure is described briefly:

Starting from either an intermediate (having only real vibrational frequencies) or an adduct of the type $[M(OH_2)_6 \cdot OH_2]^{n+}$ a selected M−O bond was elongated or compressed and kept fixed while all the other internal coordinates were optimized. The calculation was done at C_1 symmetry; the starting structure must not have a higher symmetry, otherwise corresponding distortions have to be made. Such constrained optimizations were performed for several values of the selected M−O bond until all the gradients were <0.005 hartree/bohr. The structure fulfilling these requirements was then submitted to a frequency computation. All these calculations were performed with a smaller basis set (SV quality was sufficient in this case). Finally, the transition states were located by following the appropriate mode with a negative Eigenvalue, and this calculation was performed with the large basis set.

Acknowledgment. I wish to thank Professor Dr. M. W. Schmidt for a copy of the GAMESS program system and for his helpful discussions. I also wish to thank Professor Dr. A. E. Merbach for his valuable discussions and Professors Drs. A. E. Merbach, J. Weber, and Dr. R. Humphry-Baker for their helpful comments on the manuscript.

JA960184A

(16) Swaddle, T. W. *Adv. Inorg. Bioinorg. Mech.* **1989**, *2*, 95.
(17) Swaddle, T. W. *Inorg. Chem.* **1983**, *22*, 2663.
(18) Swaddle, T. W.; Mak, M. K. S. *Can. J. Chem.* **1983**, *61*, 473.
(19) Swaddle, T. W. *Inorg. Chem.* **1980**, *19*, 3203.
(20) Schmidt, M. W.; Baldridge, K. K.; Boatz, J. A.; Elbert, S. T.; Gordon, M. S.; Jensen, J. H.; Koseki, S.; Matsunaga, N.; Nguyen, K. A.; Su, S. J.; Windus, T. L.; Dupuis, M.; Montgomery, J. A. *J. Comput. Chem.* **1993**, *14*, 1347.
(21) Baerends, E. J.; Ellis, D. E.; Ros, P. *Chem. Phys. 2* **1973**, 41. te Velde, G.; Baerends, E. J. *J. Comput. Phys.* **1992**, *99*, 84.
(22) Vosko, S. H.; Wilk, L.; Nusair, M. *Can. J. Phys.* **1980**, *58*, 1200.
(23) Becke, A. D. *Phys. Rev.* **1988**, *A38*, 3098.
(24) Perdew, J. P. *Phys Rev.* **1986**, *B33*, 8822.
(25) Stevens, W. J.; Krauss, M.; Basch, H.; Jasien, P. G. *Can. J. Chem.* **1992**, *70*, 612.
(26) (a) Hehre, W. J.; Ditchfield, R.; Pople, J. A. *J. Chem. Phys.* **1972**, *56*, 2257. (b) Ditchfield, R.; Hehre, W. J.; Pople, J. A. *J. Chem. Phys.* **1971**, *54*, 724.
(27) Schäfer, A.; Horn, H.; Ahlrichs, R. *J. Chem. Phys.* **1992**, *97*, 2571.